AIAA SciTech Forum
8–12 January 2018, Kissimmee, Florida
2018 AIAA Guidance, Navigation, and Control Conference

10.2514/6.2018-1844

Model Aided Estimation of Angle of Attack, Sideslip Angle, and 3D Wind without Flow Angle Measurements

Pengzhi Tian[1], Haiyang Chao[2]

Accurate estimations of the relative movement of the aircraft with respect to the surrounding air are critical to flight performance and aircraft safety. This paper proposes two novel aircraft-model-aided extended Kalman filters (EKFs), a 2-state EKF and a 9-state EKF. The proposed filters can estimate angle of attack, sideslip angle, and 3D wind without using direct flow angle measurements such as a multi-hole pitot-tube or mechanical vanes. Both simulation and small unmanned aerial vehicle (UAV) flight test data are used to validate the methods. Experimental results show that the 2-state EKF can estimate angle of attack (AOA) and angle of sideslip (AOS) with around 2 degrees root mean square errors under aggressive maneuvers compared with a high-fidelity 5-hole pitot tube. The 9-state EKF can estimate 3D wind velocities with comparable mean values as a sonic wind anemometer from a ground weather station.

Nomenclature

AOA/α	=	angle of attack
AOS/β	=	angle of sideslip
a_x, a_y, a_z	=	acceleration in aircraft body frame
b	=	wingspan
C_L	=	lift coefficient
C_Y	=	side force coefficient
$\bar{c}$	=	mean chord length
EKF	=	extended Kalman filter
GPS	=	global positioning system
g	=	acceleration due to gravity
IMU	=	inertial measurement unit
INS	=	inertial navigation system
L	=	lift
m	=	mass of aircraft
p, q, r	=	body-axis roll, pitch, and yaw rates
$\bar{q}$	=	dynamic pressure
S	=	wing area
T	=	thrust
UAV	=	unmanned aerial vehicle
UKF	=	unscented Kalman filter
u, v, w	=	body-axis air-relative velocity components
$\boldsymbol{u}$	=	input vector
V	=	true airspeed
V_g	=	GPS total ground speed
V_n, V_e, V_d	=	GPS ground speed in north, east, and down
V_{pitot}	=	pitot tube airspeed
V_w	=	wind speed

[1] Ph.D. student, Aerospace Engineering Department, University of Kansas, Lawrence, KS, 66045, (E): pengzhitian@ku.edu.
[2] Assistant Professor, Aerospace Engineering Department, University of Kansas, Lawrence, KS, 66045, (E): chaohaiyang@ku.edu.

w_n, w_e, w_d = wind speed in north, east, and down
$\boldsymbol{x}$ = state vector
Y = side force
$\boldsymbol{y}$ = output vector
$\boldsymbol{z}$ = measurement vector
$\delta_e, \delta_a, \delta_r$ = elevator, aileron, and rudder deflections
ρ = air density
ϕ, θ, ψ = Euler roll, pitch, and yaw angles

I. Introduction

The interaction between an aircraft and the surrounding flow field is crucial to flight performance and aircraft safety. There are three important parameters that describe the relative movement of the aircraft with respect to the surrounding air, which are airspeed, angle of attack (AOA) and angle of sideslip (AOS), also known as air triplets. Accurate estimations of these parameters are critical to the aircraft system identification [1,2] and potential fault detection. Meanwhile, if accurate measurements of surrounding flow field are provided, flight trajectories of an aircraft can be planned more efficiently [3].

Compared with general aviation, small unmanned aerial vehicles (UAVs) are more vulnerable to strong wind and turbulence due to their smaller size and lighter weight. On one hand, the presence of dynamic wind creates many challenges in the control of UAVs. On the other hand, small UAVs can potentially benefit from certain types of wind fields such as thermal wind or wake vortex [4,5,6] if they can be sensed or predicted accurately. Wind impact is a critical factor for safe and efficient integration of small UAVs into next generation national airspace. Accurate estimation of air flow angles and the surrounding wind field can greatly improve the flight performance as well as flight safety of UAVs. These estimates can be used in many UAV safety related applications such as stall warning, gust alleviation, collision avoidance, and air traffic control. In addition to flight safety, flight efficiency is another major factor that needs to be considered. Energy harvesting [7] and trajectory optimization [3] are two important scenarios for UAVs. To achieve safe and efficient flight, it is essential to get real-time information regarding aircraft-flow interaction. However, due to the spatial-temporal character of wind, it is very difficult to get such information during flight.

There are several existing works on estimation of air flow angles and wind velocities. Langelaan showed in simulation that 3D wind can be calculated directly by using wind triangulation [8]. Johansen proposed a Kalman filter based cascaded structure for estimation of airflow angles and wind velocities. In this approach, aircraft attitude is estimated first or assumed available, then flow angles and wind velocities are estimated using kinematic relationships [9]. Cho presented a simple extended Kalman filter (EKF) for estimation of air flow angles and 2D horizontal wind [10]. Rhudy developed an unscented Kalman filter (UKF) that estimates aircraft attitude, 3D wind with the help of AOA and AOS vanes [11]. Lie took use of the full aircraft dynamic model, inertial measurement unit (IMU), and global positioning system (GPS) measurements to estimate air triplets as well as 2D horizontal wind [12]. Wenz showed in the simulation that turbulence wind velocities, AOA, AOS, and aerodynamic coefficients can be estimated by using an EKF that combines frequency separation, kinematic, dynamic, and wind models [13]. However, many of existing approaches focused only on 2D horizontal wind. For 3D wind estimation, high quality IMU and GPS, direct flow angle measurements, wind model, or sophisticated aircraft dynamic models are generally required, which may not be available to most low-cost UAVs.

This paper presents two novel model-aided EKFs for the estimation of flow angles $[\alpha\ \beta]$ and 3D wind $[w_n\ w_e\ w_d]$ without using direct flow angle measurements. A simple aircraft aerodynamic model is used together with GPS, IMU, and 1D pitot tube measurements to form the estimation filters. These two model-aided EKFs can be applied under different scenarios. For example, the 2-state EKF can be incorporated in most commercial or open source autopilot without changing the original software structures whereas the 9-state EKF can be used when the interaction between aircraft and surrounding flow field is of great interest. The proposed filters are validated through both simulation and flight test data.

The organization of this paper can be summarized as follows. The problem of air flow angles and 3D wind estimation is formulated in Section II. The model aided EKFs proposed are presented in Section III. Then, the experimental UAV platform is introduced in detail in Section IV. Simulation and flight test results are further presented in Section V and Section VI, respectively. Finally, conclusions are made in Section VII.

II. Problem Definition

The goal of this paper is to estimate AOA, AOS, and 3D wind velocities without using direct flow angle measurements. AOA and AOS describe the angles between the aircraft body frame and wind frame [14], which can be obtained by installing flow vanes or multi-hole pitot tubes on the aircraft. Once AOA and AOS are known, 3D wind can be calculated by using the wind triangle equation with the measurements from GPS, IMU, and pitot tube [8]. Airflow angle definitions and wind triangulation are shown in Fig. 1. The direct calculation technique has been proved to work well on manned aircraft. However, due to the limited payload and budget of small UASs, direct measurements may not be available or not accurate enough for direct calculation using wind triangle equation.

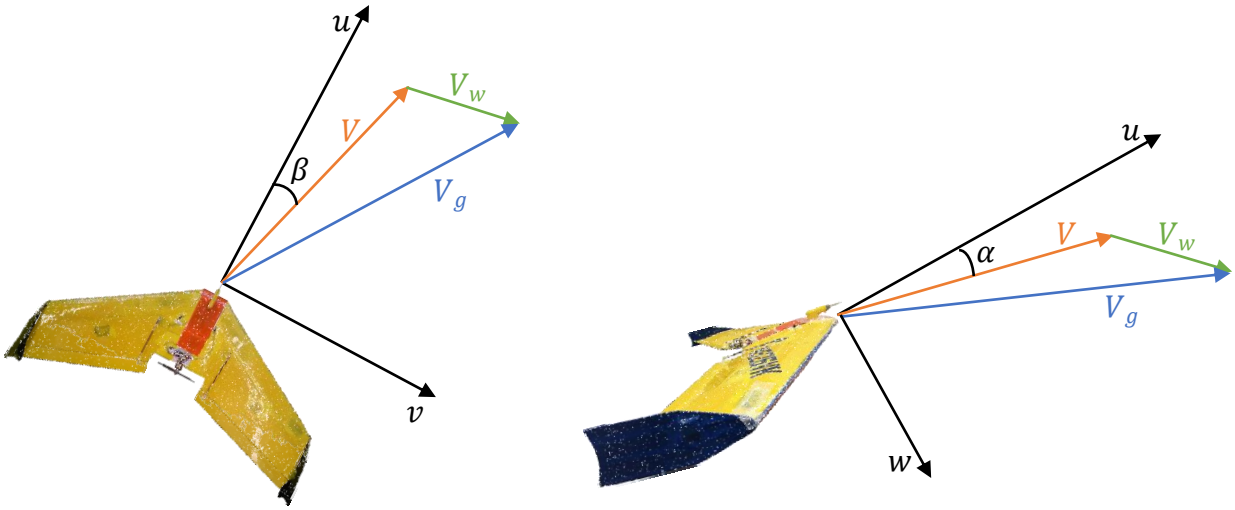

Figure 1. Airflow Angles and Wind Triangulation.

In this paper, estimations of angle of attack, sideslip angle, and 3D wind are studied with standard sensor suites widely available on small UASs, which include GPS, IMU, and 1D pitot tube. For different applications and sensor qualities, various forms of filters can be used. This paper presents two filters with a simple form (2-state EKF) and an extensive form (9-state EKF).

1. Euler angles $[\phi\ \theta\ \psi]$ are available with high quality; the objective is to estimate flow angles $[\alpha\ \beta]$. In this case, Euler angles $[\phi\ \theta\ \psi]$ are considered as inputs of the system. Other required inputs include accelerations $[a_x\ a_y\ a_z]$, angular rates $[p\ q\ r]$, and pitot tube measured airspeed $[V_{pitot}]$. Aircraft aerodynamic model parameters required are lift coefficients (C_L) and side force coefficients (C_Y). Outputs of the system are flow angles $[\alpha\ \beta]$.
2. Euler angles $[\phi\ \theta\ \psi]$ are not available or with low quality; the objective is to estimate air triplets $[V\ \alpha\ \beta]$ and 3D wind $[w_n\ w_e\ w_d]$. In this case, inputs of the system are accelerations $[a_x\ a_y\ a_z]$, angular rates $[p\ q\ r]$, pitot tube measured airspeed $[V_{pitot}]$, and GPS ground speed $[V_n\ V_e\ V_d]$. The required aircraft aerodynamic model parameters are lift coefficients (C_L) and side force coefficients (C_Y). Outputs of the system are air triplets $[V\ \alpha\ \beta]$, 3D wind $[w_n\ w_e\ w_d]$, and Euler angles $[\phi\ \theta\ \psi]$.

III. Model Aided Extended Kalman Filters

Kalman filter is the most commonly used method for combining noisy measurements from multiple sensors. Given corrupted data from GPS, IMU, and pitot tube, EKFs can be used for attitude, wind velocity, and air triplets estimation. Two model-aided EKFs proposed are introduced in detail in this section.

A. 2-State EKF

The 2-state EKF developed in this paper can estimate AOA and AOS purely based on inertial measurements and pitot tube airspeed. The filter is performed through the fusion of IMU measurements of accelerations $[a_x\ a_y\ a_z]$, angular rates $[p\ q\ r]$, Euler angles $[\phi\ \theta\ \psi]$, pitot tube measurement $[V_{pitot}]$, and aircraft lift and side force

coefficients. To estimate AOA and AOS using EKF, two sets of equations are required, which are propagation equations and update equations. The propagation equations of the EKF are given by Eq. (1) and (2) [15].

$$\dot{\alpha} = q + \frac{g\cos\phi\cos\theta\cos\alpha + g\sin\theta\sin\alpha - a_x\sin\alpha + a_z\cos\alpha}{V\cos\beta} - (p\cos\alpha + r\sin\alpha)\tan\beta \tag{1}$$

$$\dot{\beta} = \frac{1}{V}\left[\left(-a_x\cos\alpha\sin\beta + a_y\cos\beta - a_z\sin\alpha\sin\beta\right) + g(\sin\theta\cos\alpha\sin\beta + \cos\theta\sin\phi\cos\beta - \cos\theta\cos\phi\sin\alpha\sin\beta)\right] + p\sin\alpha - r\cos\alpha \tag{2}$$

These two equations are derived by differentiating the definition equations of AOA and AOS and substituting aircraft body-axis velocity equations and aircraft force equations [16]. The update equations are given by Eq. (3) and (4), which are derived from aircraft lift and side force equations shown in Eqs. (5)~(7).

$$C_{L_0} + C_{L_{\delta e}}\delta_e + \frac{C_{L_q}q\bar{c}}{(2V)} = \frac{m(a_x\sin\alpha - a_z\cos\alpha) - T\sin\alpha}{\bar{q}S} - C_{L_\alpha}\alpha \tag{3}$$

$$\frac{\frac{ma_y}{\bar{q}S} - C_{Y_0} - \frac{C_{Y_p}pb}{(2V)} - \frac{C_{Y_r}rb}{(2V)} - C_{Y_{\delta a}}\delta_a - C_{Y_{\delta r}}\delta_r}{C_{Y_\beta}} = \beta \tag{4}$$

According to the force equation, lift equals to the projection of gravity and thrust

$$L = m(a_x\sin\alpha - a_z\cos\alpha) - T\sin\alpha \tag{5}$$

Lift can also be approximated if lift coefficients are known

$$L = C_L\bar{q}S \approx \left(C_{L_0} + C_{L_\alpha}\alpha + C_{L_{\delta e}}\delta_e + C_{L_q}q\bar{c}/(2V)\right)\bar{q}S \tag{6}$$

By substituting lift from Eq. (6) in Eq. (5) and moving all α components to the right side of equation, Eq. (3) is derived.

Similarly, update equation for β can be derived by correlating side force equations shown in Eq. (7)

$$Y = ma_y = C_Y\bar{q}S \approx \left(C_{Y_0} + C_{Y_\beta}\beta + \frac{C_{Y_p}pb}{(2V)} + \frac{C_{Y_r}rb}{(2V)} + C_{Y_{\delta a}}\delta_a + C_{Y_{\delta r}}\delta_r\right)\bar{q}S \tag{7}$$

In summary, the state, input and observation vectors are given by:

$$\boldsymbol{x} = [\alpha\ \beta]^T$$

$$\boldsymbol{u} = \left[a_x\ a_y\ a_z\ p\ q\ r\ \phi\ \theta\ V_{pitot}\right]^T$$

$$\boldsymbol{y} = \begin{bmatrix} C_{L_0} + C_{L_{\delta e}}\delta_e + \frac{C_{L_q}q\bar{c}}{(2V)} \\ \frac{\frac{ma_y}{\bar{q}S} - C_{Y_0} - \frac{C_{Y_p}pb}{(2V)} - \frac{C_{Y_r}rb}{(2V)} - C_{Y_{\delta a}}\delta_a - C_{Y_{\delta r}}\delta_r}{C_{Y_\beta}} \end{bmatrix}$$

B. 9-State EKF

The 9-state EKF developed in this paper considers the simultaneous estimation of aircraft body-axis velocity components $[u\ v\ w]$, Euler angles $[\phi\ \theta\ \psi]$, and wind velocity components $[w_n\ w_e\ w_d\ ]$ in the north-east-down (NED) inertial frame. This filter requires the knowledge of aircraft lift and side force coefficients, GPS ground velocities $[V_n\ V_e\ V_d]$, accelerations $\left[a_x\ a_y\ a_z\right]$ and rotation rates $[p\ q\ r]$ from IMU, and 1D pitot tube measurement $\left[V_{pitot}\right]$.

The propagation equation of this EKF is derived from equations of translational and rotational motion of an aircraft which is given by Eq. (8) [11]

$$\dot{\boldsymbol{x}} = \begin{bmatrix} \dot{u} \\ \dot{v} \\ \dot{w} \\ \dot{\phi} \\ \dot{\theta} \\ \dot{\psi} \\ \dot{w}_n \\ \dot{w}_e \\ \dot{w}_d \end{bmatrix} = \begin{bmatrix} -qw + rv - gsin\theta + a_x \\ -ru + pw + gcos\theta sin\phi + a_y \\ -pv + qu + gcos\theta cos\phi + a_z \\ p + tan\theta(qsin\phi + rcos\phi) \\ qcos\phi - rsin\phi \\ (qsin\phi + rcos\phi)/cos\theta \\ 0 \\ 0 \\ 0 \end{bmatrix} \tag{8}$$

In this equation, the wind dynamics are modeled as random walk processes. During implementation, Gaussian noise terms are added after the equation is discretized, thus the equation for $[\dot{w}_n\ \dot{w}_e\ \dot{w}_d]^T$ is showing as $[0\ 0\ 0]^T$ here.

The measurements from the pitot tube and GPS as well as aircraft lift and side force are used in the update equation as correctors. The update equation is a combination of the wind triangle equation, calculations of triplets from the body-axis velocity components, and aircraft lift/side force equations given by

$$\boldsymbol{y} = \begin{bmatrix} V_n \\ V_e \\ V_d \\ V_{pitot} \\ C_{L_0} + C_{L_{\delta e}}\delta_e + \frac{C_{L_q} q\bar{c}}{(2V)} \\ \frac{\frac{ma_y}{\bar{q}S} - C_{Y_0} - \frac{C_{Y_p} pb}{(2V)} - \frac{C_{Y_r} rb}{(2V)} - C_{Y_{\delta a}}\delta_a - C_{Y_{\delta r}}\delta_r}{C_{Y_\beta}} \end{bmatrix} = \begin{bmatrix} ucos\psi cos\theta + v(-sin\psi cos\phi + cos\psi sin\theta sin\phi) + v(sin\psi sin\phi + cos\psi sin\theta cos\phi) + w_n \\ usin\psi cos\theta + v(cos\psi cos\phi + sin\psi sin\theta sin\phi) + v(-cos\psi sin\phi + sin\psi sin\theta cos\phi) + w_e \\ -usin\theta + vcos\theta sin\phi + vcos\theta cos\phi + w_d \\ u \\ \frac{m\left(a_x \frac{\mathrm{w}}{\sqrt{u^2+w^2}} - a_z \frac{u}{\sqrt{u^2+w^2}}\right) - T\frac{\mathrm{w}}{\sqrt{u^2+w^2}}}{\frac{\rho(u^2+v^2+w^2)S}{2}} - C_{L_\alpha} \tan^{-1}\left(\frac{w}{u}\right) \\ sin^{-1}\left(v/\sqrt{u^2+v^2+w^2}\right) \end{bmatrix} \tag{9}$$

Notice that in Eq. (9), $[V\ \alpha\ \beta]$ are expressed in the form of aircraft body-axis velocity components $[u\ v\ w]$ by using the definition equations shown in Eq. (10) [14]. After getting $[u\ v\ w]$ from the estimation, $[V\ \alpha\ \beta]$ can be calculated using Eq. (10).

$$V = \sqrt{u^2 + v^2 + w^2}$$

$$\alpha = \tan^{-1}\left(\frac{w}{u}\right) \tag{10}$$

$$\beta = \sin^{-1}\left(\frac{v}{V}\right)$$

In summary, the state, input and observation vectors are given by:

$$\boldsymbol{x} = [u\ v\ w\ \phi\ \theta\ \psi\ w_n\ w_e\ w_d]^T$$

$$\boldsymbol{u} = \left[a_x\ a_y\ a_z\ p\ q\ r\right]^T$$

$$\boldsymbol{y} = \begin{bmatrix} V_n \\ V_e \\ V_d \\ V_{pitot} \\ C_{L_0} + C_{L_{\delta e}}\delta_e + \frac{C_{L_q} q \bar{c}}{(2V)} \\ \frac{ma_y}{\bar{q}S} - C_{Y_0} - \frac{C_{Y_p} pb}{(2V)} - \frac{C_{Y_r} rb}{(2V)} - C_{Y_{\delta a}}\delta_a - C_{Y_{\delta r}}\delta_r \\ C_{Y_\beta} \end{bmatrix}$$

IV. Experimental Platform

KHawk 55'' UAV, shown in Fig. 2, was used for the data collection. General specifications of the UAV are shown in Table 1. KHawk 55" UAV supports both manual remote controlled mode and autonomous mode. The airborne avionics includes a Microstrain GX3 IMU, a u-blox GPS receiver, a 900 MHz data modem, a Gumstix computer, an open source Paparazzi autopilot, and an air data system. One of the two optional air data systems can be installed for air flow measurements including one low-cost Eagle Tree airspeed system (air speed only), and one Aeroprobe 5-hole air data system (airspeed, AOA, and AOS). The 5-hole pitot-tube setup is shown in the right of Fig. 2 with the standalone unit shown in Fig. 3. The Eagle Tree air data system is shown in Fig. 4 with customized 3D print parts for pitot-tube mounting. All the sensor data is logged onboard the aircraft including inertial data (100Hz), GPS data (4 Hz), air flow data (50Hz for EagleTree sensor or 100 Hz for Aeropobe sensor). It is worth mentioning that the Aeroprobe 5-hole pitot-tube has an airspeed range of 8-45 m/s and AOA/AOS range of -20-20 degrees. In other words, the Aeroprobe pitot-tube will not report a meaningful value when operating outside of the calibrated range.

Figure 2. KHawk 55'' UAV Platform.

Figure 3. Five-Hole Pitot Tube from Aeroprobe.

Table 1. KHawk 55" UAV specifications.

UAS Parameter	Specifications
Take-off Weight	~ 2.5 kg
Max Payload	0.5 kg
Material	EPOR Foam, Carbon Spar
Wingspan	1.4 meters (55 inches)
Control Mode	Elevons
Engine	Pusher Brushless Motor
Endurance	~ 45 minutes
Cruise Speed	20 m/s
Take-off	Bungee

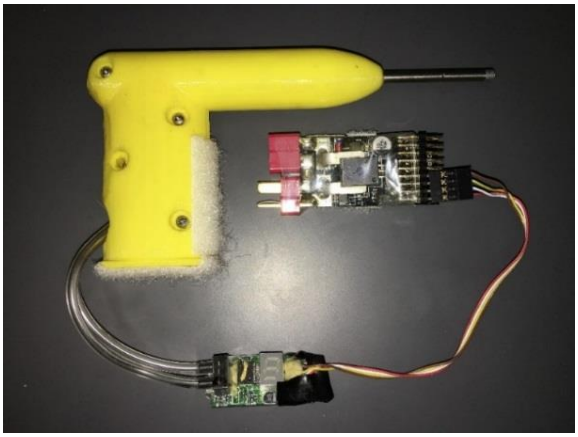

Figure 4. Eagle Tree V3 Airspeed Sensor.

Lift coefficients (C_L) and side force coefficients (C_Y) of the KHawk 55'' UAV were identified through flight test by using least square method [17]. Identified coefficients are shown in Table 2.

Table 1. KHawk 55'' UAV Lift and Side Force Coefficients

C_{L_0}	$C_{L_\alpha}\left(\frac{1}{rad}\right)$	$C_{L_q}\left(\frac{s}{rad}\right)$	$C_{L_{\delta_e}}\left(\frac{1}{rad}\right)$	C_{Y_0}	$C_{Y_\beta}\left(\frac{1}{rad}\right)$	$C_{Y_p}\left(\frac{s}{rad}\right)$	$C_{Y_r}\left(\frac{s}{rad}\right)$	$C_{Y_{\delta_a}}\left(\frac{1}{rad}\right)$
0.0563	1.8789	0.1796	0.8297	0.0037	-0.25	0	0.0123	0.0351

In order to validate wind estimation results, the UAV was flown at the field, where a weather station is installed, shown in Fig. 5. The weather station is approximately 3 meters off the ground, which can provide 3D wind measurements at 20 Hz.

Figure 5. Weather Station.

V. Simulation Results

Simulation results are focused in this section for the validation of the developed filters in the presence of sensor noises. The 6-DOF aircraft simulator was used, based on MATLAB Flight Dynamics and Control (FDC) toolbox. More details can be found in [15].

The first simulation is to validate the 2-state EKF. During the simulation, elevator doublet (around 10 seconds) and aileron doublet (around 12 seconds) inputs were used to excite changes in α and β. Gaussian noises were added to system inputs $[a_x\ a_y\ a_z\ p\ q\ r\ \phi\ \theta\ V_{pitot}]$ based on noise characteristics from real sensors. AOA, and AOS estimations are shown in Fig. 6.

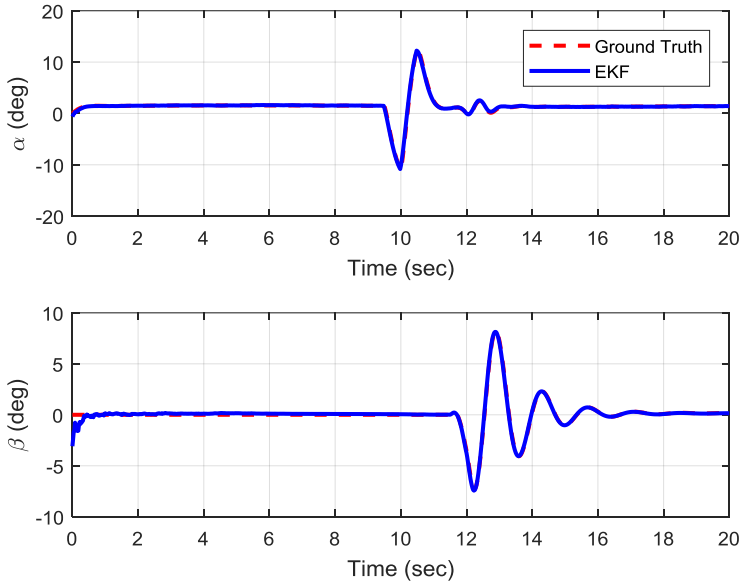

Figure 6. 2-State EKF AOA/AOS Estimation vs. Ground Truth.

The second simulation is to validate the 9-state EKF. During the simulation, the aircraft is commanded to circle down. However, there are some oscillations due to the presence of wind disturbance. The north, east, down winds are set to 6 m/s, -5 m/s, and 1 m/s, respectively. Gaussian noises are added to system inputs $[a_x\ a_y\ a_z\ p\ q\ r]$ as well as measured outputs $[V_n\ V_e\ V_d\ V_{pitot}]$ based on noise characteristics from real sensors. The attitude estimation results are

shown in Fig. 7. Airspeed, AOA, and AOS estimations are shown in Fig. 8. Both attitude and air triplets are estimated accurately despite the presence of sensor noises.

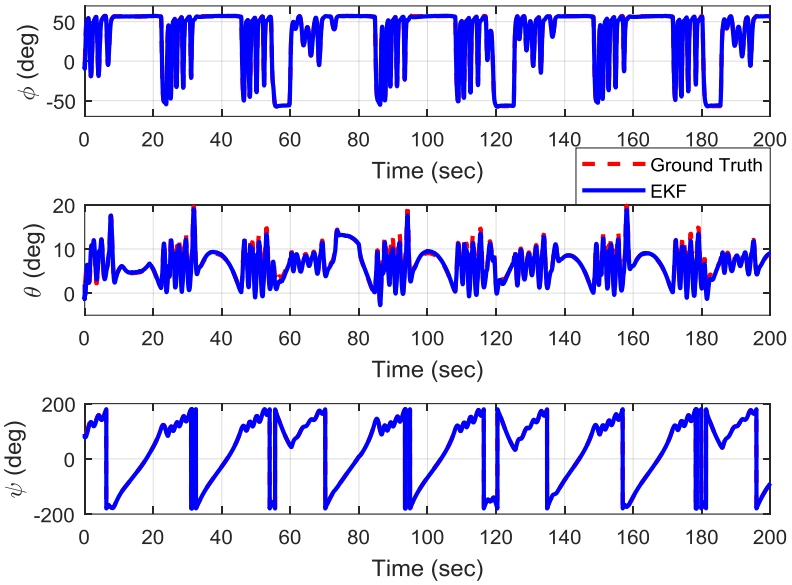

Figure 7. 9-State EKF Attitude Estimation vs. Ground Truth.

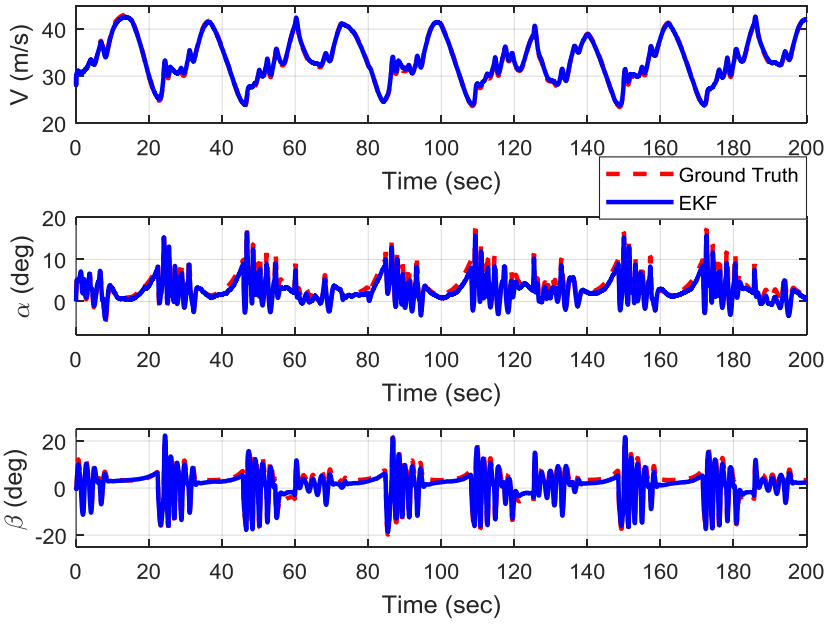

Figure 8. 9-State EKF Air Triplets Estimation vs. Ground Truth.

3D wind estimation results are shown in Fig. 9. It can be observed that north and east wind velocities are estimated with an accuracy of less than 0.3 m/s, however, the downwind estimation has around 1 m/s static error, which needs to be further studied in the future.

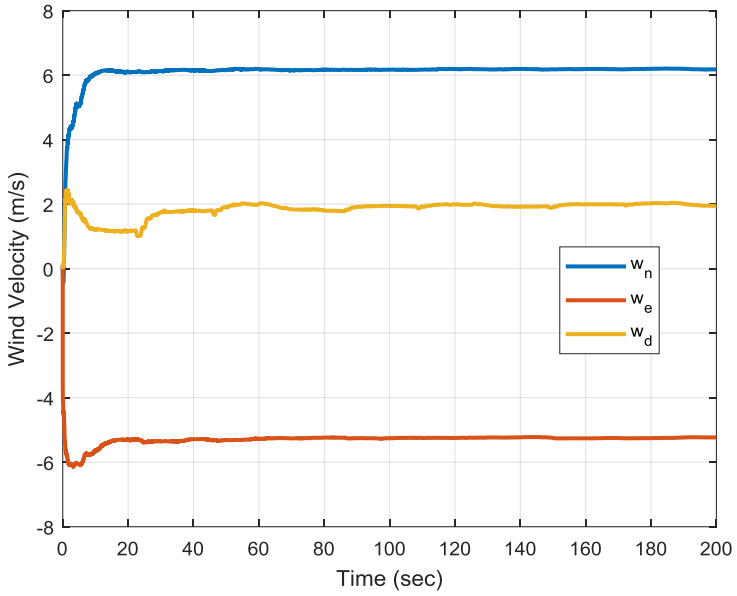

Figure 9. 9-State EKF 3D Wind Estimation.

VI. UAV Flight Test Results

Two sets of flight data were used in this study, which were collected by the KHawk 55'' UAV on different days. The thrust is currently ignored in both filters as it is observed in simulation that the results are similar with or without thrust components.

The first data set was collected in a calm day with a five-hole pitot tube installed, providing high quality AOA and AOS. During the flight, the aircraft was chirped at different frequencies to excite both AOA and AOS. The 2-state EKF is implemented to estimate AOA and AOS, shown in Fig. 10 along with five-hole pitot tube measurements. The zoomed in result is shown in Fig. 11. Statistical analysis of estimation results are shown in Table 3.

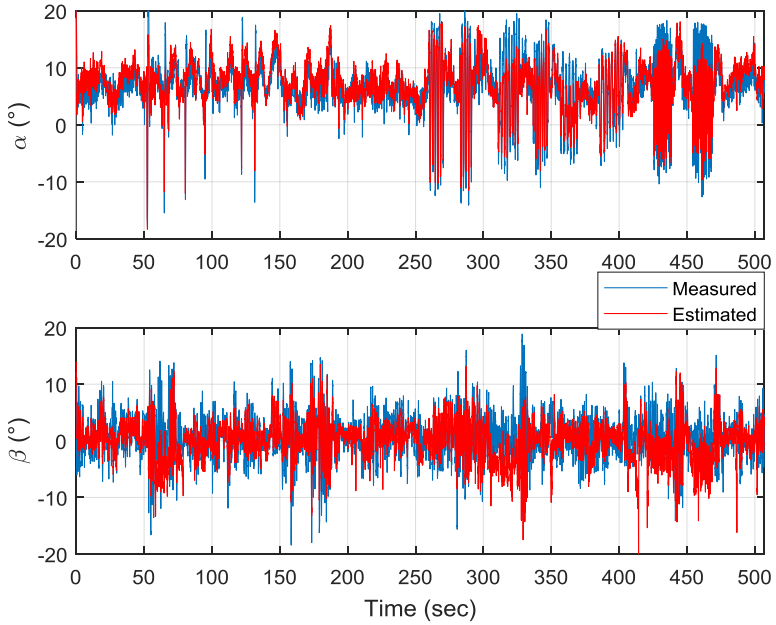

Figure 10. Estimated AOA/AOS vs. Five-Hole Pitot Tube Measurements.

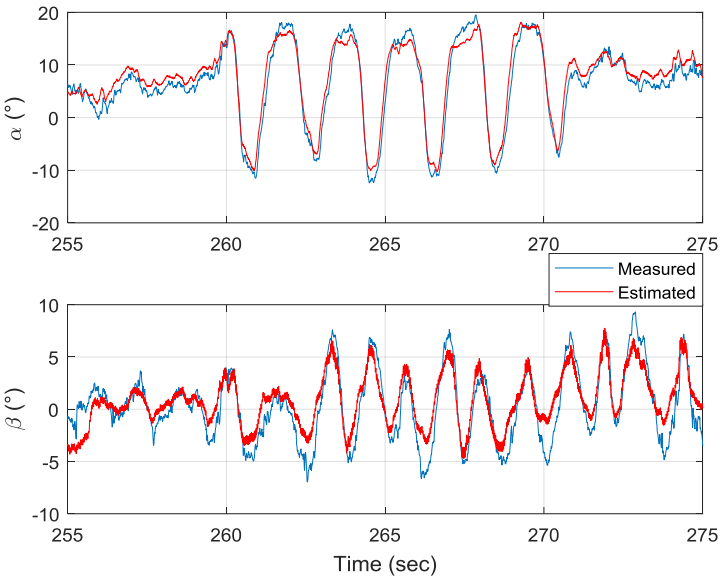

Figure 11. Zoomed in Estimated AOA/AOS vs. Five-Hole Pitot Tube Measurements.

Table 3. Statistical Analysis of 2-State EKF Estimation Results

AOA mean error (°)	AOA error std. (°)	AOS mean error (°)	AOS error std. (°)
1.8805	1.3643	2.0384	2.1030

The second data set was collected with an Eagle Tree V3 airspeed sensor installed. The flight test was conducted at the University of Kansas Field Station, where a weather station can provide 3D wind measurements at 20 Hz. The 9-state EKF is implemented to simultaneous estimate aircraft body-axis velocity components $[u\ v\ w]$, Euler attitude angles $[\phi\ \theta\ \psi]$, and wind velocities $[w_n\ w_e\ w_d\ ]$ in the north-east-down (NED) inertial frame. AOA and AOS are calculated by using Eq. (10) after getting the estimation of $[u\ v\ w]$. Due to the lack of direct measurements of flow angles, only estimated AOA and AOS are shown in Fig. 12.

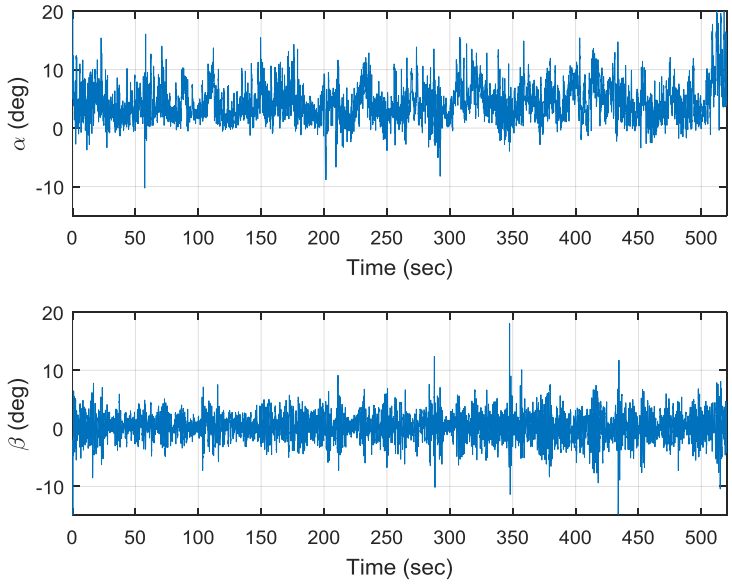

Figure 12. Estimated AOA/AOS Using 9-State EKF.

Estimations of 3D wind are shown in Fig. 13 along with weather station measurements. It takes the 9-state EKF roughly 50 seconds to converge. Once converged, the estimation results show a good match with measurements from weather station.

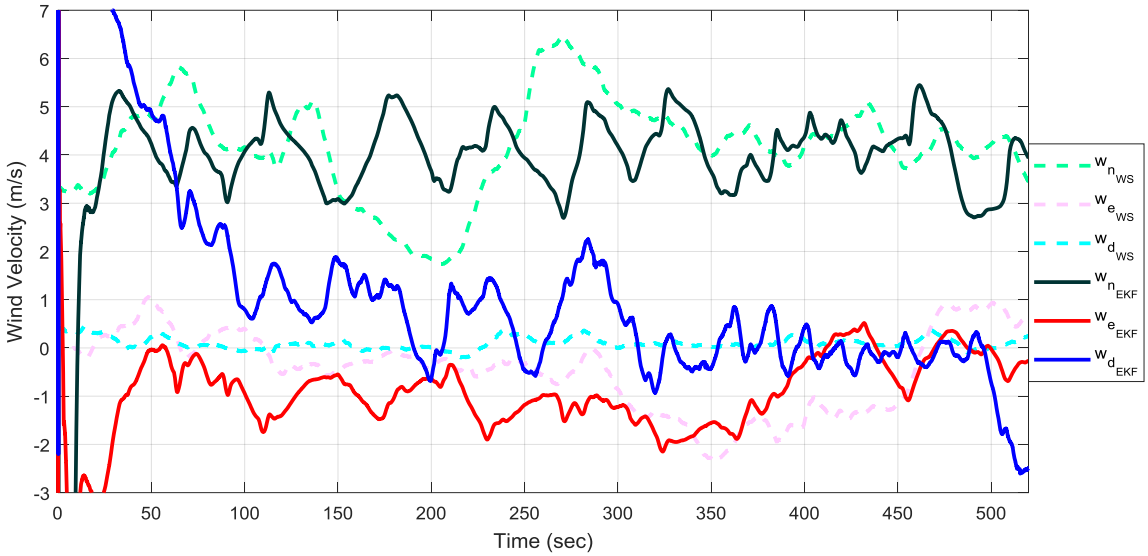

Figure 13. Estimated 3D Wind Using 9-State EKF vs. Weather Station Measurements.

VII. Conclusions

In this paper, two model-aided EKFs (2-state EKF and 9-state EKF) are developed without using direct flow angle measurements. These two filters can be applied under different scenarios based on applications and sensor qualities. Both filters are validated through simulations with presence of realistic sensor noises. The UAV flight test data further showed the effectiveness of 2-state EKF and 9-state EKF for the estimation of flow angles as well as 3D wind. Future works will focus on the improvement of estimation accuracy and reconstruction of dynamic 3D wind fields such as wind shear and fire generated turbulence.

Acknowledgments

The authors would like to thank Dr. Nathaniel A. Brunsell for providing weather station data and Dr. Dean Kettle from Kansas Biological Survey for the help with flight test. This work was partially supported by NASA grant #NNX14AF55A and the University of Kansas General Research Fund allocation #2221800.

References

[1] Morelli, E. A., "Real-time Aerodynamic Parameter Estimation without Air Flow Angle Measurements," Journal of Aircraft, Vol. 49, No. 4, 2012, pp. 1064-1074.

[2] Jategaonkar, R. V., "Flight Vehicle System Identification: A Time Domain Methodology," Vol. 216, Progress in Astronautics and Aeronautics, AIAA, 2006.

[3] Lawrance, N. R. J., and Sukkarieh, S., "Wind Energy Based Path Planning for a Small Gliding Unmanned Aerial Vehicle," AIAA Guidance, Navigation, and Control Conference, 2009.

[4] Vachon, M. J., Ray, R. J., Walsh, K. R., and Ennix, K., "F/A-18 Aircraft Performance Benefits Measured During the Autonomous Formation Flight Project," AIAA Atmospheric Flight Mechanics Conference, 2002.

[5] Pahle, J., Berger, D., Venti, M., Duggan, C., Faber, J., and Cardinal, K., "An Initial Flight Investigation of Formation Flight for Drag Reduction on the C-17 Aircraft," AIAA Atmospheric Flight Mechanics Conference, 2012.

[6] Chao, H., Gu, Y., Tian, P., Zheng, Z., and Napolitano, M., "Wake Vortex Detection with UAV Close Formation Flight," AIAA Atmospheric Flight Mechanics Conference, 2015.

[7] Langelaan, J. W., Montella, C, and Grenestedt, J., "Wind Field Estimation for Autonomous Dynamic Soaring," IEEE International Conference on Robotics and Automation, 2012.

[8] Langelaan, J., Alley, N., and Neidhoefer, J., "Wind Field Estimation for Small Unmanned Aerial Vehicles," Journal of Guidance, Control, and Dynamics, Vol. 34, No. 4, 2011, pp. 1016-1030.

[9] Johansen, T. A., Cristofaro, A., Srensen, K., Hansen, J. M., and Fossen, T. I., "On Estimation of Wind Velocity, Angle of Attack and Sideslip Angle of Small UAVs Using Standard Sensors," International Conference on Unmanned Aircraft Systems, 2015.

[10] Cho, A., Kim, J., Lee, S., and Kee, C., "Wind Estimation and Airspeed Calibration using a UAV with a Single-Antenna GPS Receiver and Pitot Tube," IEEE Trans. on Aerospace and Electronic Systems, Vol. 47, No. 1, 2011, pp. 109-117.

[11] Rhudy, M., Larrabee, T., Chao, H., Gu, Y., and Napolitano, M. R., "UAV Attitude, Heading, and Wind Estimation Using GPS/INS and an Air Data System," AIAA Guidance, Navigation, and Control Conference, 2013.

[12] F. A. P. Lie and D. Gebre-Egziabher, "Synthetic air data system," Journal of Aircraft, vol. 50, No. 4, 2013, pp. 1234–1249.

[13] Wenz, A., Johansen, T.A. and Cristofaro, A., "Combining Model-Free and Model-Based Angle of Attack Estimation for Small Fixed-Wing UAVs Using a Standard Sensor Suite," International Conference on Unmanned Aircraft Systems (ICUAS), 2016.

[14] Beard, R. W., and McLain, T. W., Small Unmanned Aircraft: Theory and Practice, Princeton University Press, 2012.

[15] Rauw, M. O., "FDC 1.2-A Simulink Toolbox for Flight Dynamics and Control Analysis," 2011.

[16] Klein, V., and Morelli, E. A., *Aircraft System Identification—Theory and Practice*, AIAA Education Series, AIAA, Reston, VA, 2006.

[17] Chao, H., Flanagan, H. P., Tian, P., Hagerott, S. G., "Flight Test Investigation of Stall/Spin Detection Techniques for a Flying Wing UAS," AIAA Atmospheric Flight Mechanics Conference, 2017.